

AD-A189 617

AUTOMATED STEREOPHOTOGRAMMETRY(U) VIRGINIA POLYTECHNIC
INST AND STATE UNIV BLACKSBURG DEPT OF ELECTRICAL
ENGINEER RING M NADLER 10 DEC 87 ARO-22476.3-GS

1/1

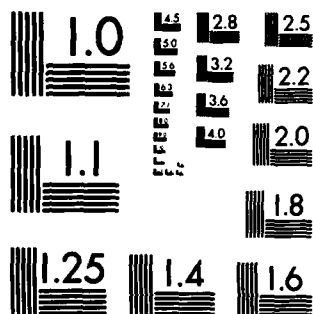
UNCLASSIFIED

DAAG29-85-K-0250

F/G 8/2

NL

END
PAGE
8



MICROCOPY RESOLUTION TEST CHART
NATIONAL BUREAU OF STANDARDS-1963-A

UNCL/
SECURITY

AD-A189 617

DTIC FILE COPY ②

DOCUMENTATION PAGE

1a. REPORT SECURITY CLASSIFICATION Unclassified		1b. RESTRICTIVE MARKINGS	
2a. SECURITY CLASSIFICATION AUTHORITY		3. DISTRIBUTION/AVAILABILITY OF REPORT Approved for public release; distribution unlimited.	
2b. DECLASSIFICATION/DOWNGRADING SCHEDULE		5. MONITORING ORGANIZATION REPORT NUMBER(S) ARO 22476.3-65	
4. PERFORMING ORGANIZATION REPORT NUMBER(S)			
6a. NAME OF PERFORMING ORGANIZATION Bradley Dept. of Electrical Eng'g VPI&SU		6b. OFFICE SYMBOL (If applicable)	
7a. NAME OF MONITORING ORGANIZATION U. S. Army Research Office		7b. ADDRESS (City, State, and ZIP Code) P. O. Box 12211 Research Triangle Park, NC 27709-2211	
6c. ADDRESS (City, State, and ZIP Code) Blacksburg VA 24061-0111		7c. ADDRESS (City, State, and ZIP Code) P. O. Box 12211 Research Triangle Park, NC 27709-2211	
8a. NAME OF FUNDING/SPONSORING ORGANIZATION U. S. Army Research Office		8b. OFFICE SYMBOL (If applicable)	
9. PROCUREMENT INSTRUMENT IDENTIFICATION NUMBER DAA629-85-K-0250		10. SOURCE OF FUNDING NUMBERS	
8c. ADDRESS (City, State, and ZIP Code) P. O. Box 12211 Research Triangle Park, NC 27709-2211		PROGRAM ELEMENT NO. PROJECT NO. TASK NO. WORK UNIT ACCESSION NO.	
11. TITLE (Include Security Classification) Automated Stereophotogrammetry (Unclassified)			
12. PERSONAL AUTHOR(S) Morton Nadler			
13a. TYPE OF REPORT Final		13b. TIME COVERED FROM 9/18/85 TO 9/17/87	
14. DATE OF REPORT (Year, Month, Day) 12/10/87		15. PAGE COUNT 20	
16. SUPPLEMENTARY NOTATION The view, opinions and/or findings contained in this report are those of the author(s) and should not be construed as an official Department of the Army position, policy, or decision, unless so designated by other documentation.			
17. COSATI CODES		18. SUBJECT TERMS (Continue on reverse if necessary and identify by block number)	
FIELD	GROUP	SUB-GROUP	Stereophotogrammetry, Pattern Recognition, Topological Method, Hexagonal scan array
19. ABSTRACT (Continue on reverse if necessary and identify by block number) Using a pattern recognition approach, we have developed a fast program for finding characteristic points and calculating disparities in pairs of photographs. The procedure derives oriented edge-vector graphs from the photos, locates singular points (nodes) in the graphs, and then tests a small window about these points for match. In common with other window-matching approaches, the procedure uses a coarse-to-fine analysis, where the averaged blocks in the coarse resolutions are staggered to simulate a hexagonal array. This enables us to take advantage of the unique topological properties of such arrays. Under a slow image processing environment (GIPSY on VAX 11/785) a dense network of matched points was obtained at the rate of 5 pts/s, compared to 15 pts/s at ETL on a CYBER-730. The ETL procedure required interactive priming with a certain number of initial matches. Since our procedure does not require initial priming, we estimate that this algorithm is at least an order of magnitude faster than the one in current use.			
20. DISTRIBUTION/AVAILABILITY OF ABSTRACT <input type="checkbox"/> UNCLASSIFIED/UNLIMITED <input type="checkbox"/> SAME AS RPT. <input type="checkbox"/> DTIC USERS		21. ABSTRACT SECURITY CLASSIFICATION Unclassified	
22a. NAME OF RESPONSIBLE INDIVIDUAL		22b. TELEPHONE (Include Area Code) 22c. OFFICE SYMBOL	

TITLE

AUTOMATED STEREOPHOTOGRAMMETRY

TYPE OF REPORT (TECHNICAL, FINAL, ETC.)

FINAL

AUTHOR (S)

Morton Nadler

DATE

Dec. 9, 1987

U. S. ARMY RESEARCH OFFICE

CONTRACT/ GRANT NUMBER

DAAG29-85-K-0250

INSTITUTION

The Bradley Dept. of Electrical Engineering

Virginia Polytechnic Institute
and State University

Accession For	
NTIS GRA&I	<input checked="" type="checkbox"/>
DTIC TAB	<input type="checkbox"/>
Unannounced	<input type="checkbox"/>
Justification	
By	
Distribution/	
Availability Codes	
Dist	Avail and/or Special
A-1	



APPROVED FOR PUBLIC RELEASE;
DISTRIBUTION UNLIMITED.

88 1 27 157

THE VIEW, OPINIONS, AND/OR FINDINGS CONTAINED IN THIS REPORT ARE THOSE OF THE AUTHOR(S) AND SHOULD NOT BE CONSTRUED AS AN OFFICIAL DEPARTMENT OF THE ARMY POSITION, POLICY, OR DECISION, UNLESS SO DESIGNATED BY OTHER DOCUMENTATION.

Results of ARO DAAG29-85-K-0250

Automated Stereophotogrammetry

The Spatial Data Analysis Laboratory has developed a pattern recognition approach to window matching in the aerial stereophotogrammetry problem. In essence, an oriented graph based on edge vectors is extracted from the photopair and corresponding topological features -- nodes -- are tested for match. To facilitate the topological analysis the graphs are generated on a pseudo-hexagonal raster.

The results of ARO DAAG29-85-K-0250, "Automated Stereophotogrammetry were very encouraging. In particular, with a slow image processing environment (GIPSY on VAX 11/785) a dense network of matched points was obtained at the rate of 5 points/s, vs. 15 points/s at ETL on a Cyber-730.

The results of the two algorithms are very similar at most points. On the Cyber-730 ETL's routine provides a match rate of 15 pts/sec, not including the time for the interactive priming matches. Our algorithm, running on the Vax-11/785, produces a match rate of 5 pts/sec. Considering the machine differences and the additional time for interactive matching, we estimate that our algorithm is at least an order of magnitude faster than the one currently used at ETL. But, more importantly, it does not require the tedious priming of initial matches.

The present approach uses a pattern recognition technique to reduce the volume of cross-correlation computation. Essentially, the algorithm constructs a pair of oriented graphs representing visual edges in the original aerial photopair and then determines corresponding topological features in the two graphs.

The algorithm needs to be tested on further image pairs of varied nature (urban, rural, jungle, etc.). Pattern features, i.e., nodes in the directed graph generated by the algorithm, can be utilized for detection and recognition of man-made objects on the ground. This was not investigated in the research just concluded. The present proposal covers these points, among others.

Furthermore, future work on the algorithm itself could involve applications to computer vision in general. In particular, this could lead to vision systems for self-guided robot vehicles.

Outline of the Algorithm

Preliminary work was done by Nadler and Signor [1977] on an orthogonal array. In this study, their work was translated to the hexagonal array and several refinements were made to the algorithm.

The present algorithm almost completely automates the stereophotogrammetry process. It does require some preliminary coarse manual matching to choose the initial resolution on the digital gray-scale images and to roughly align them, but it does not require any interactive matching to obtain initial offsets. The algorithm refines the disparity map by matching corresponding topological features at successively finer resolutions.

The steps in the algorithm will be illustrated by figures taken from Brookshire's thesis [1987] (the figure numbers are those in the thesis; not all the figures from the thesis are reproduced here).

Figure 1 shows a gray-scale reproduction of a digitized stereopair of aerial photographs, taken over mountainous terrain. At mid-right can be seen a river running from north to south. The outline of the algorithm for four resolutions (18x18 pixels averaged into 1 pseudo-pixel, 6x6, 2x2, and the final full-resolution analysis using individual pixels) follows.

Figure 3 gives the steps in the basic algorithm, repeated at each of the resolutions except the final one. We now consider the major steps in that algorithm.

Figure 7 shows the construction of the pseudo-hexagonal tilings. Here the heavy lines represent the consolidated pseudo-pixels, the dashed lines the original pixels of the digitized image, where the consolidated pixels are simply the averaged gray values of the original pixels entering into them. The reason for using the pseudo-hexagonal tiling is for its topological properties. It has the same connectivity properties as a true hexagonal tiling [Golay, 1969].

Figure 8 shows the edge-vector calculation. In Brookshire's work the vectors were obtained from the derived orthogonal components; in the future they will be generated directly from the pseudo-hexagonal array. In the next steps the full edge-vector field is filtered using thresholding and association [Bowker, 1974, Nadler and Signor, 1977], to obtain a noisy oriented graph representing the principal features visible at the given pseudo-hex resolution (Fig. 9).

The oriented graphs are then examined for singular points -- "nodes" (Fig. 12). Because of an initial rough alignment of the two images and the successive refinement of the coordinate grids, using the disparities found at preceding resolutions, corresponding nodes are never very far from each other in the current

coordinate systems. Thus, for each pair of candidate matching nodes the full vector field in a small window about these nodes can be analyzed to verify if there is an actual match or not.

Figure 19 represents the pseudo-hex images of the terrains of Fig. 1 at resolution 18×18 . The full edge-vector field obtained from the left image is shown in Fig. 20. After filtering, we have the noisy oriented graph of Fig. 22, with the nodes indicated by the small squares in Fig. 23. Finally, nodes with confirmed matches are indicated by the small circles in Figs. 24, 25.

After calculation of the disparities and interpolating, we have the contour plot of Fig. 27. This is to be compared with the corresponding plots at resolution 6 (Fig. 32) and full resolution (using gray scale correlation matching), Fig. 33. For comparison, Fig. 34 shows the contour map of the same area from ETL. A pair of 3-d plots, the SDAL result above and the ETL result below is given in Fig. 35. They are very close, but the fractal appearance of the SDAL plot may indicate that it hews closer to the actual terrain.

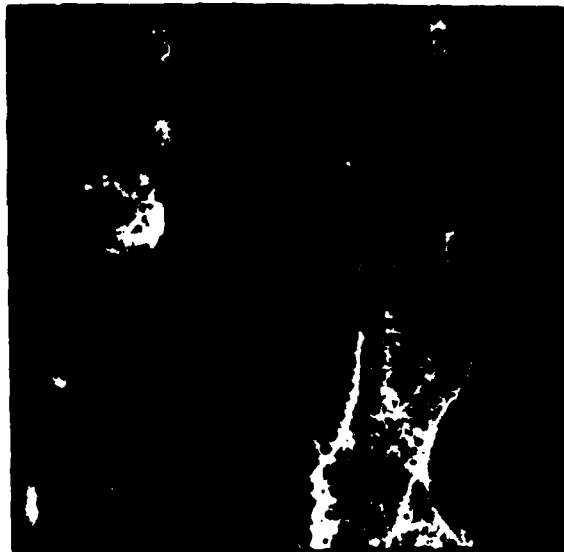
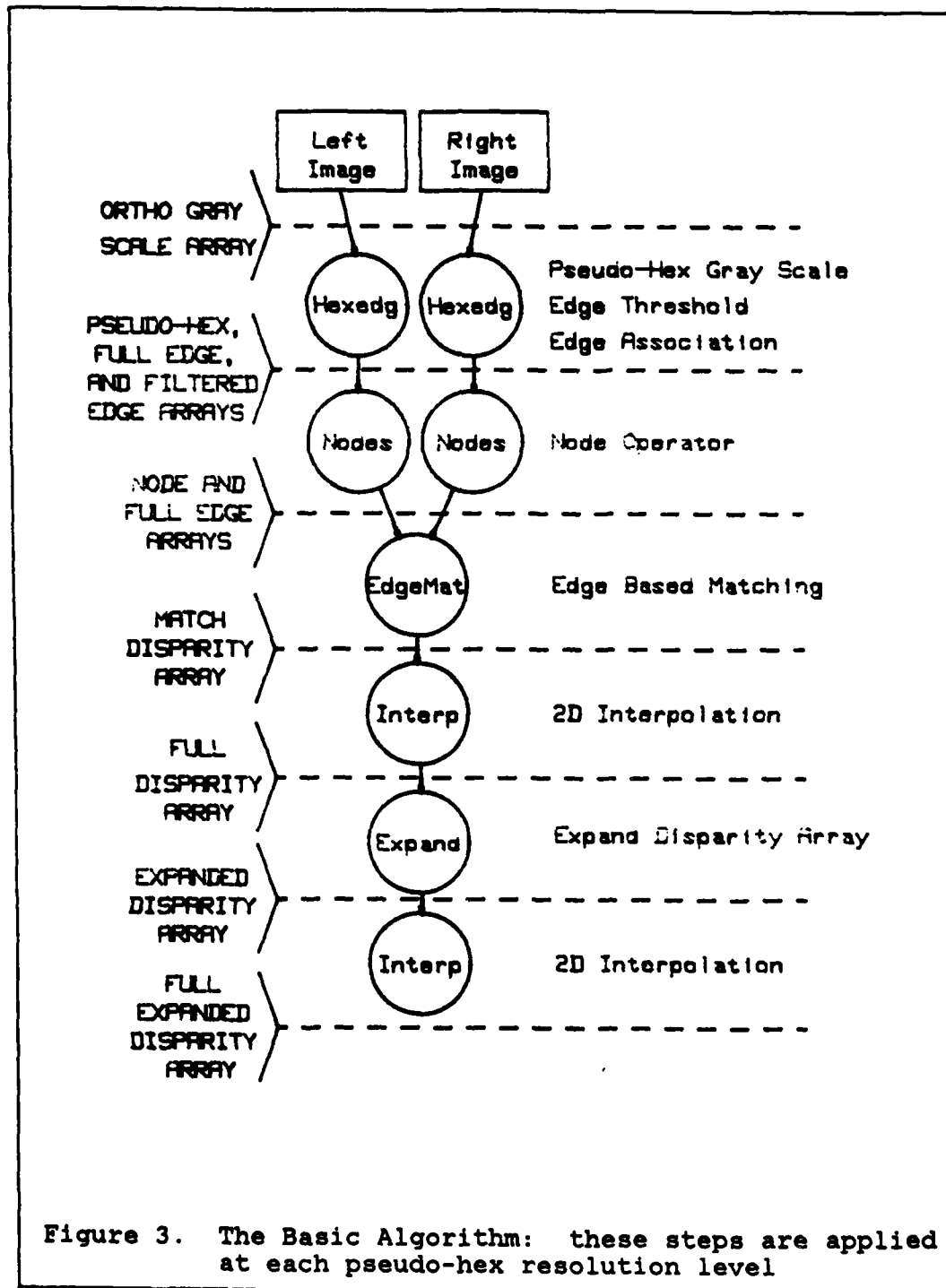
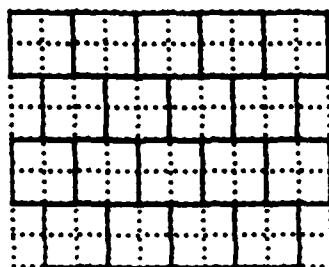
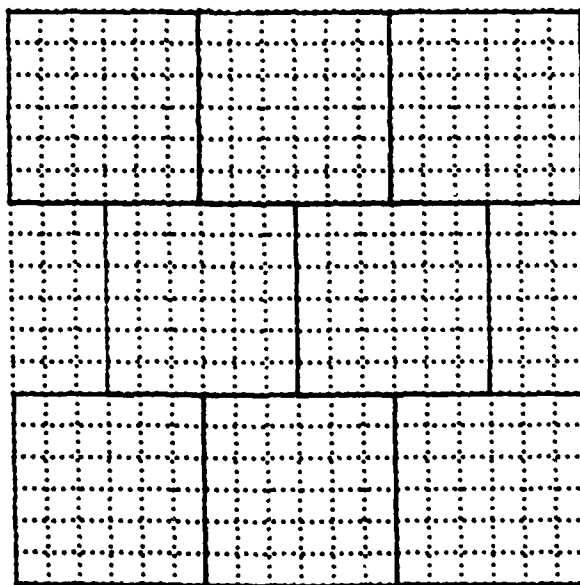


Figure 1. A Stereo Pair of Aerial Photos



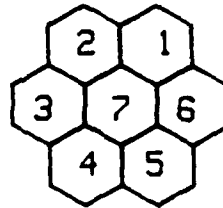


Sample Res 2 Pseudo Hex

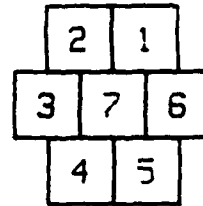


Sample Res 6 Pseudo Hex

Figure 7. The Pseudo-Hexagonal Array



Hexagonal



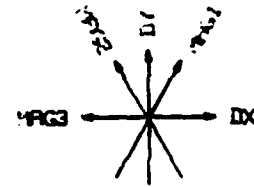
Pseudo-Hex

Hexagonal Gradient Components...

$$\text{MAG1} = \text{HEX1} - \text{HEX4}$$

$$\text{MAG2} = \text{HEX2} - \text{HEX5}$$

$$\text{MAG3} = \text{HEX3} - \text{HEX6}$$



Orthogonal Components...

$$\text{DX} = \text{MAG1} * \cos 60 - \text{MAG2} * \cos 60 - \text{MAG3}$$

$$\text{DY} = \text{MAG1} * \sin 60 + \text{MAG2} * \sin 60$$

Edge-Vector Angle and Magnitude...

$$\text{THETA} = \text{ARCTAN}(\text{DY} / \text{DX}) + 90$$

$$\text{MAG} = \text{SCR}(\text{DX}^2 + \text{DY}^2)$$

Angle Quantization...

$$-15 \leq \text{THETA} < 15$$

$$\text{DIR} = 1$$

$$15 \leq \text{THETA} < 45$$

$$\text{DIR} = 2$$

$$315 \leq \text{THETA} < -15$$

$$\text{DIR} = 12$$

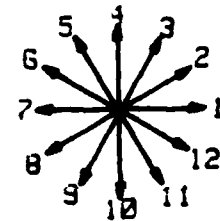
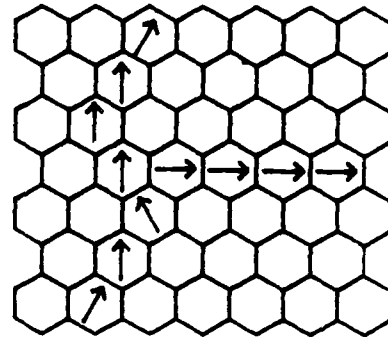
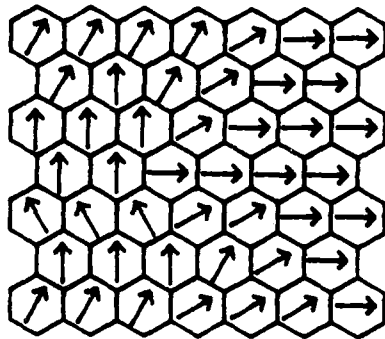
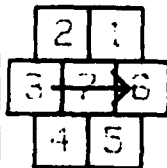


Figure 8. Edge-Vector Calculation



Case 1



$$MSUM0 = M7 + 1/2 (M3 + M5)$$

$$MSUM1 = M1 + M2$$

$$MSUM2 = M4 + M5$$

RETAINED IF

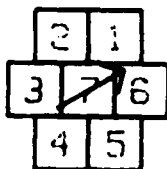
$$MSUM0 \geq MSUM1 * \text{MAX} (\cos (D7 - D1),$$

$$\text{AND} \cos (D7 - D2))$$

$$MSUM0 \geq MSUM2 * \text{MAX} (\cos (D7 - D4),$$

$$\cos (D7 - D5))$$

Case 2



$$MSUM0 = M7 + 1/4 (M1 + M3 + M4 + M5)$$

$$MSUM1 = M2 + 1/2 (M1 + M3)$$

$$MSUM2 = M5 + 1/2 (M4 + M6)$$

RETAINED IF

$$MSUM0 \geq MSUM1 * \cos (D7 - D2)$$

AND

$$MSUM0 \geq MSUM2 * \cos (D7 - D5)$$

Figure 9. Vector Association Filter

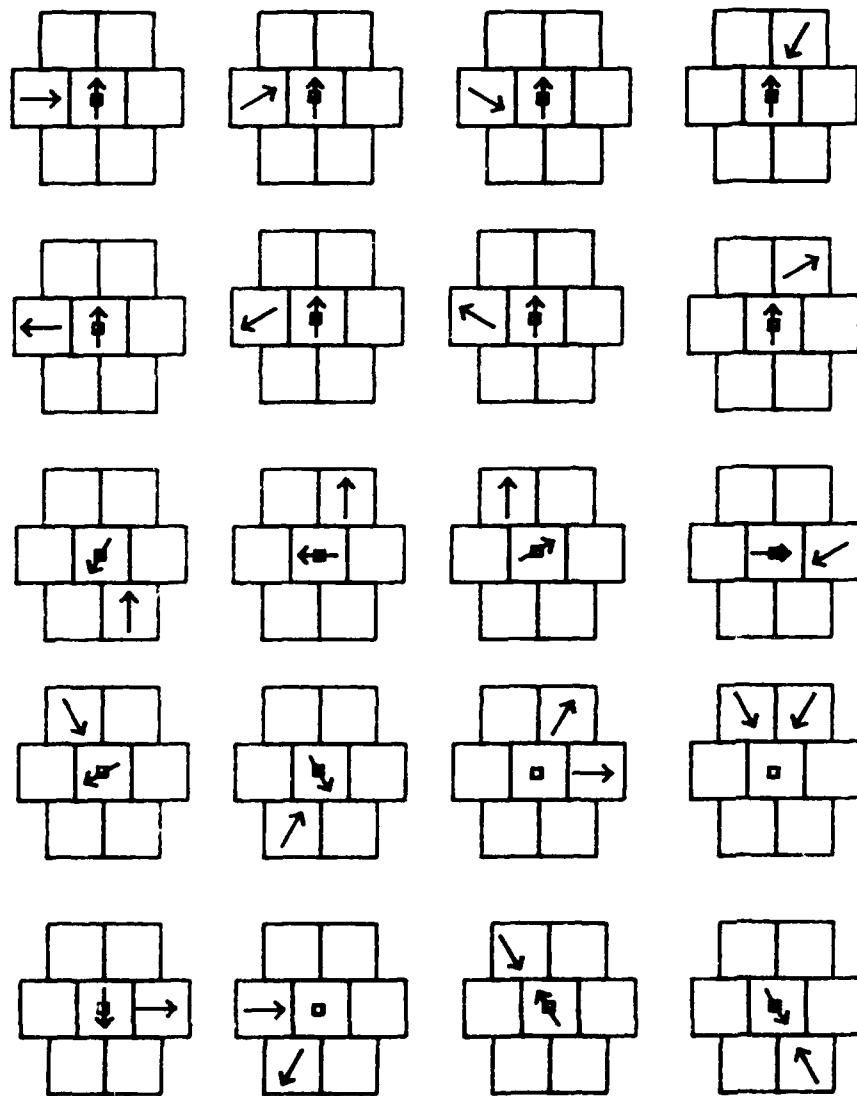


Figure 12. Examples of Nodes

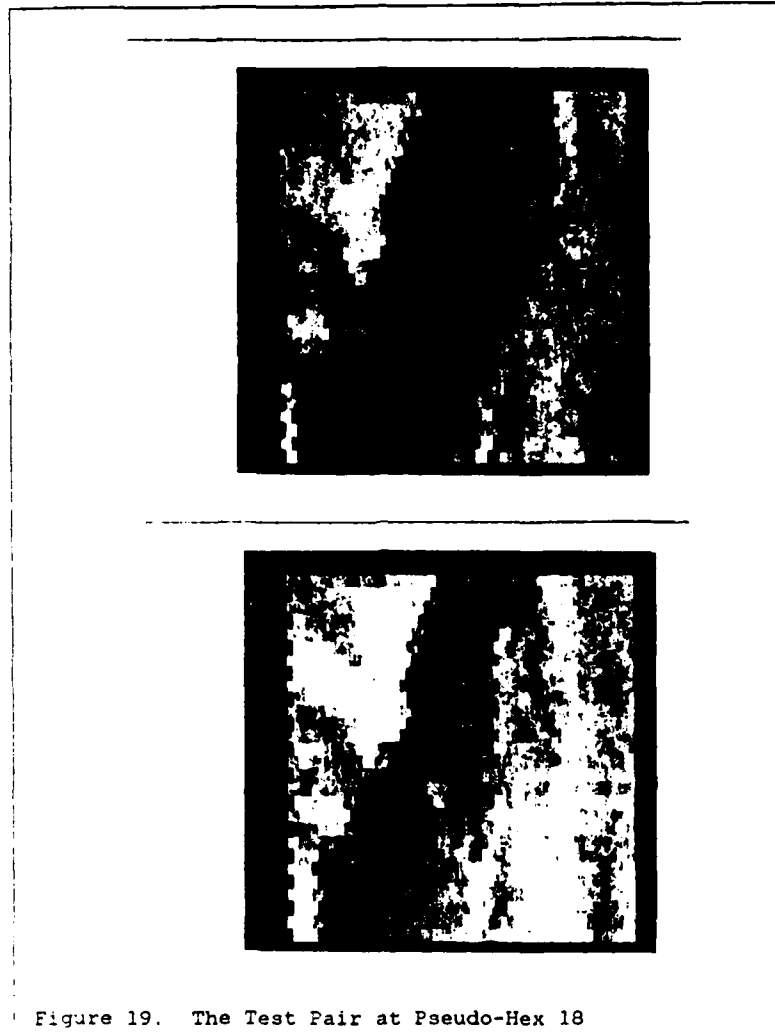


Figure 19. The Test Pair at Pseudo-Hex 18

Results

58

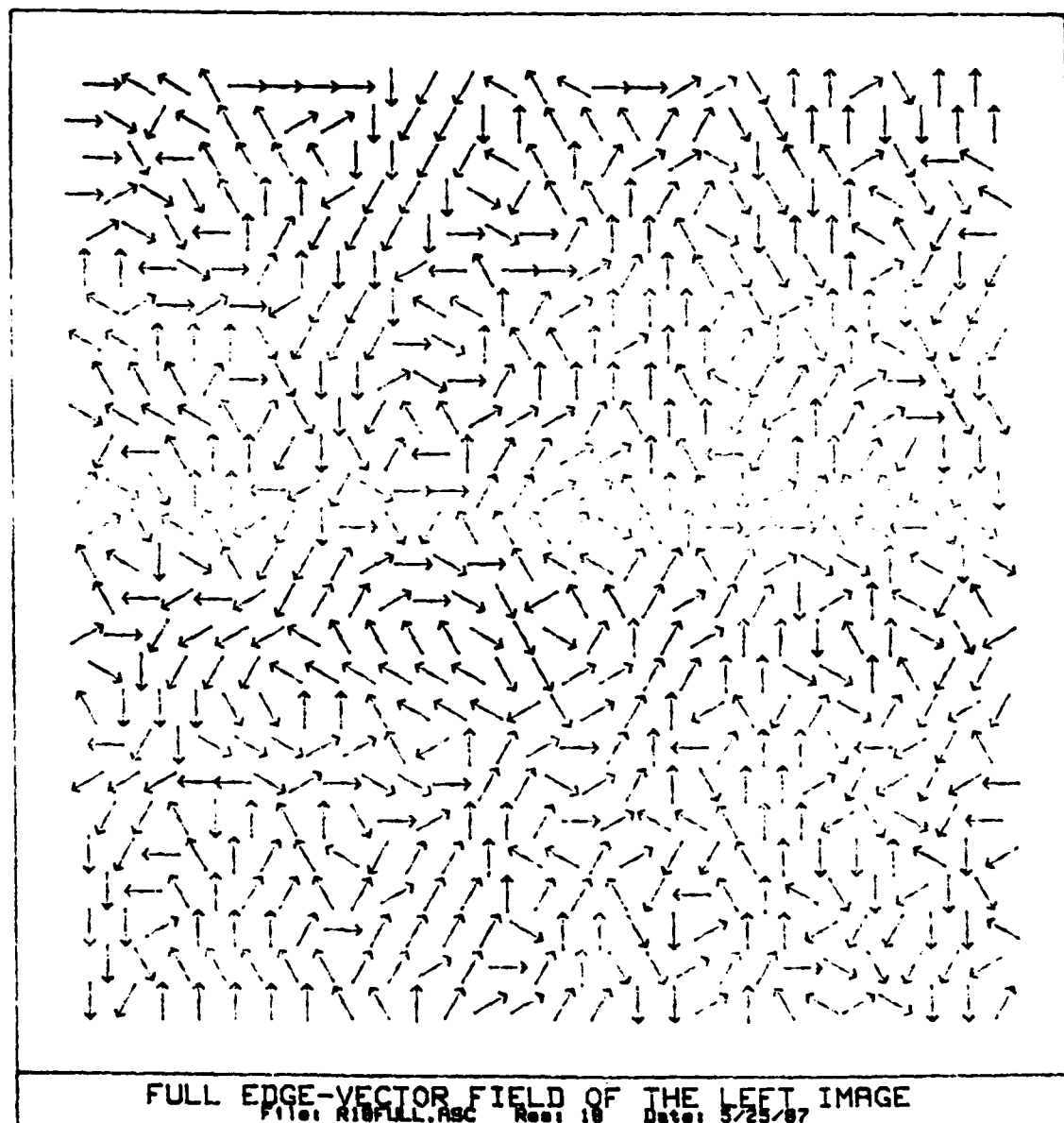


Figure 20. The Full Edge Field

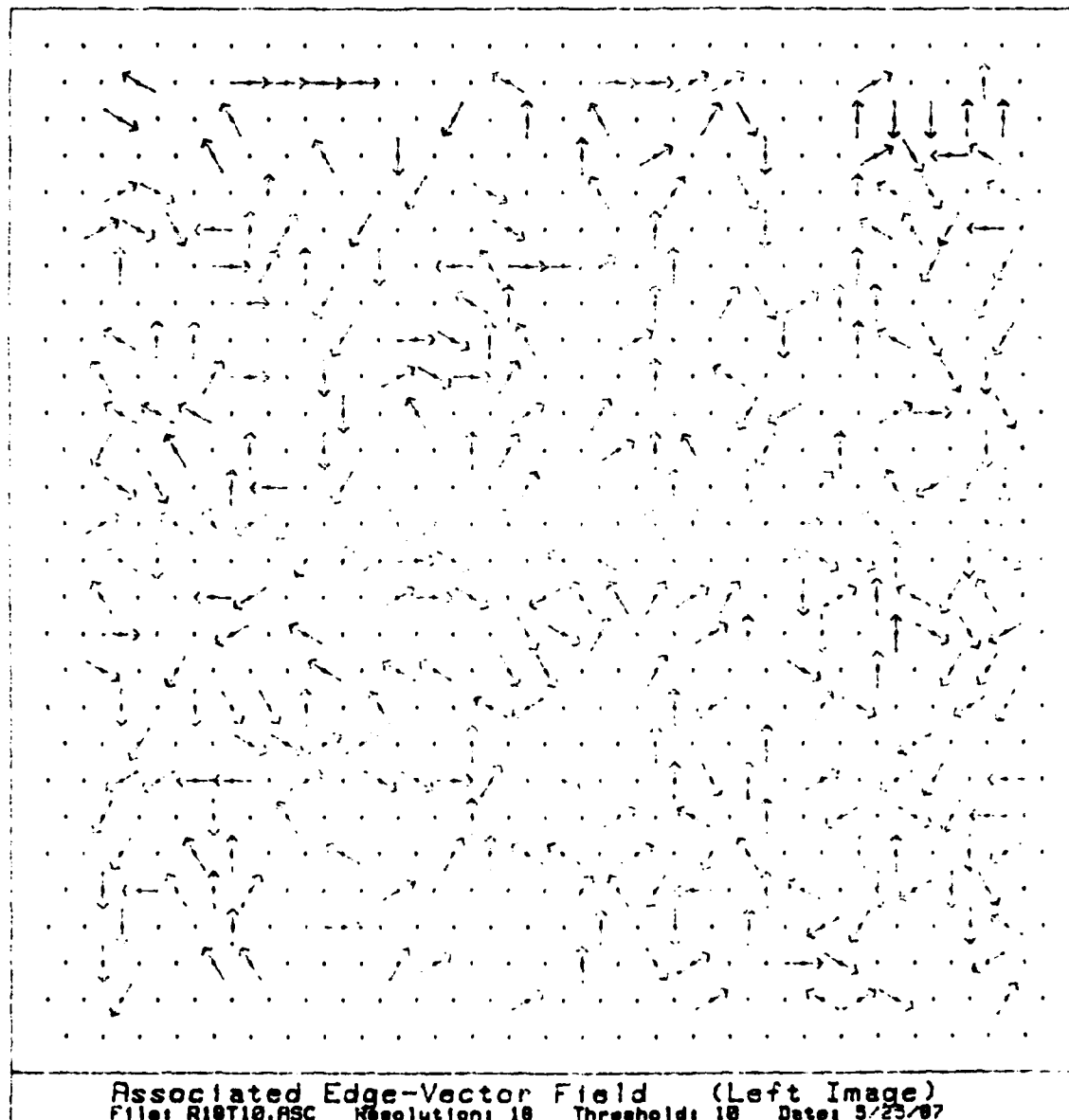


Figure 22. Associated Edge Field

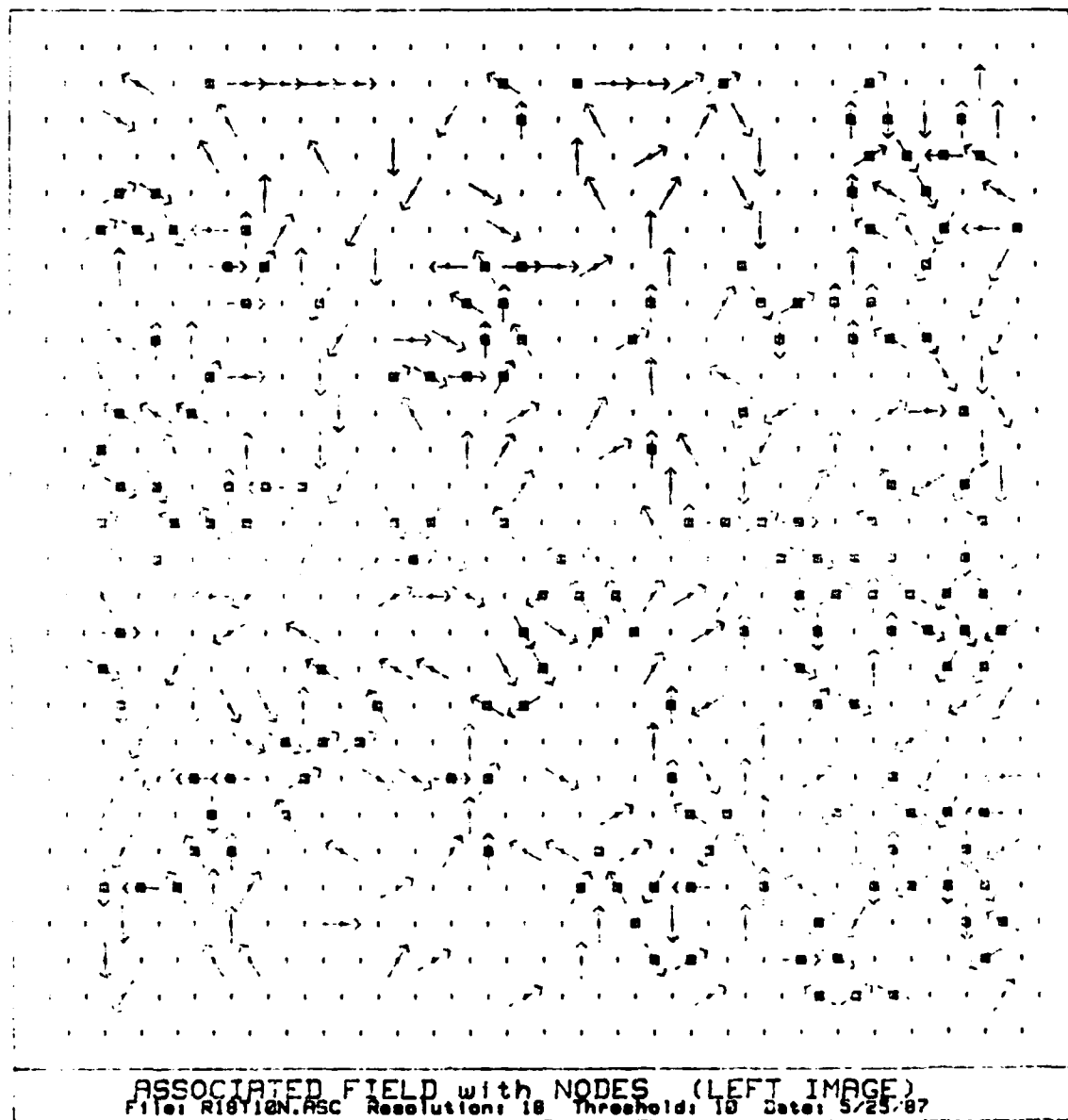


Figure 23. Nodes on the Associated Edges

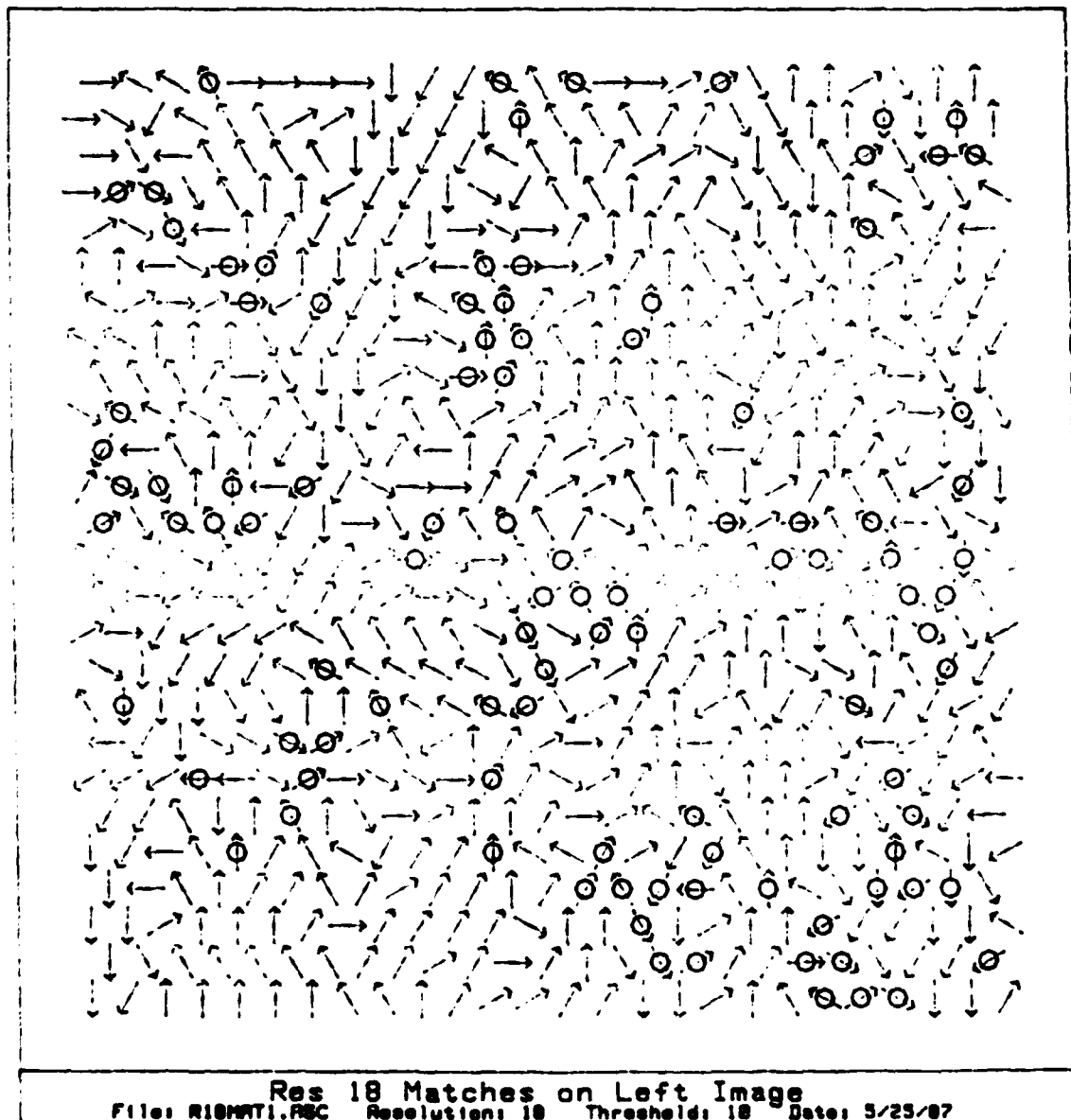


Figure 24. Matches on Image 1

Results

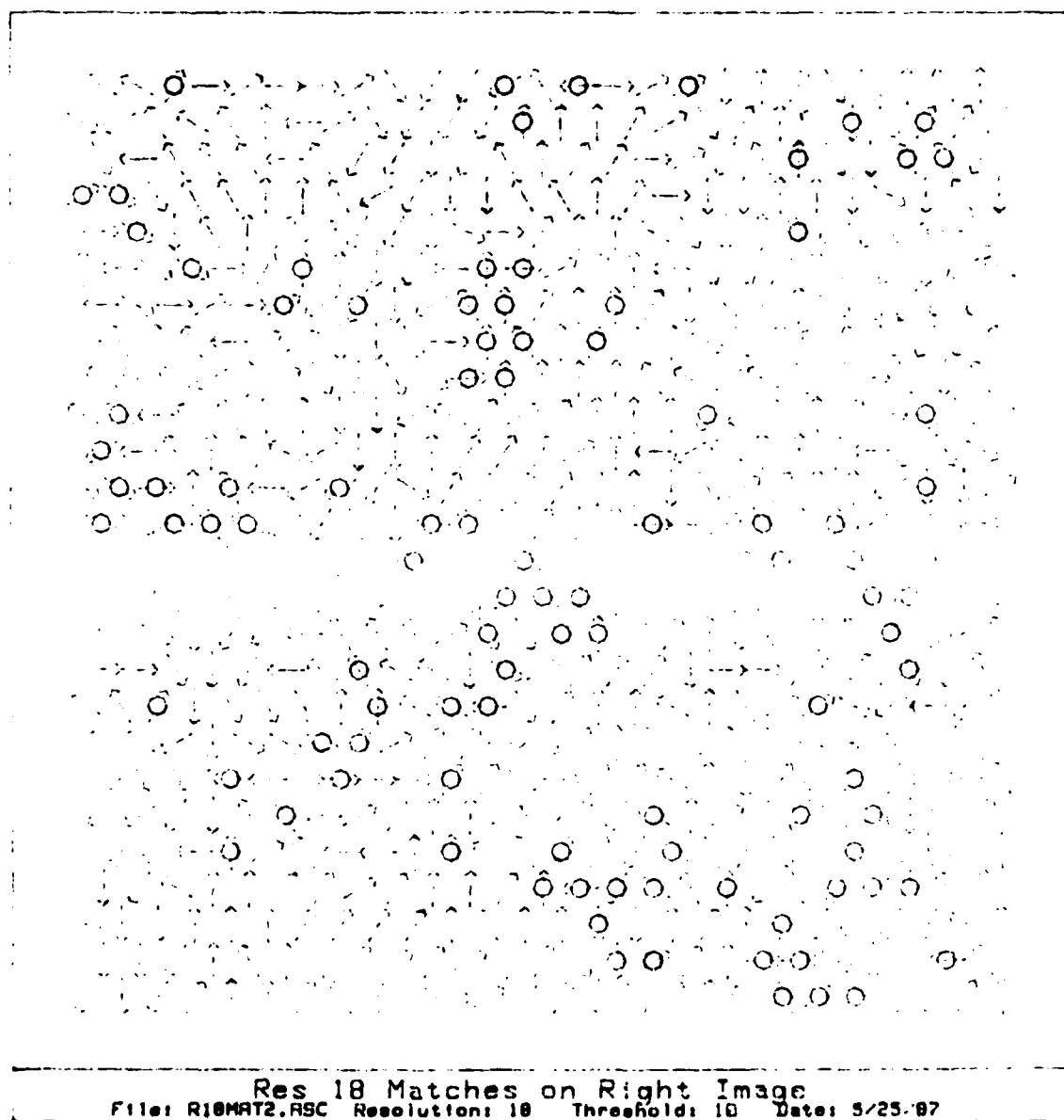
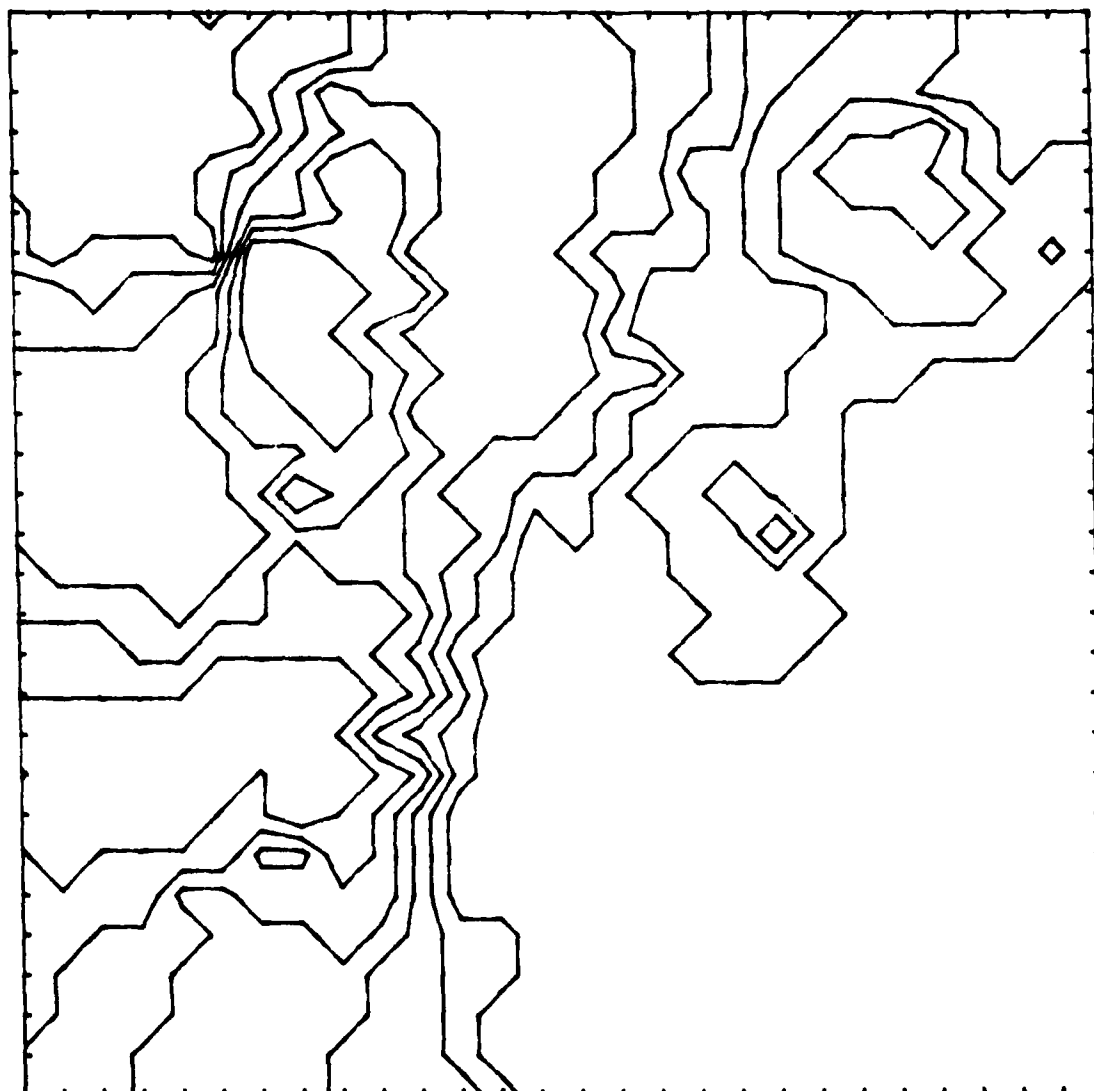
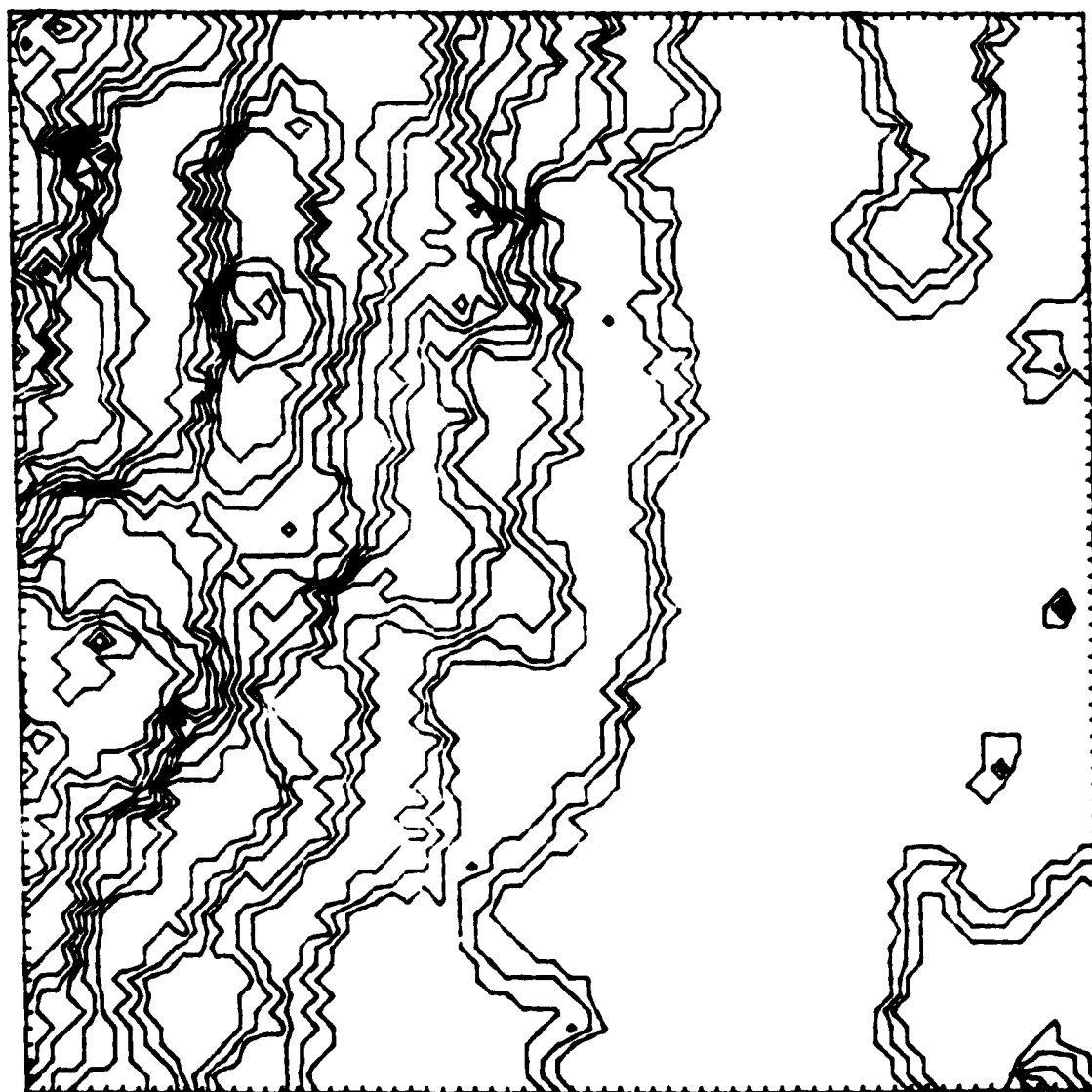


Figure 25. Matches on Image 2



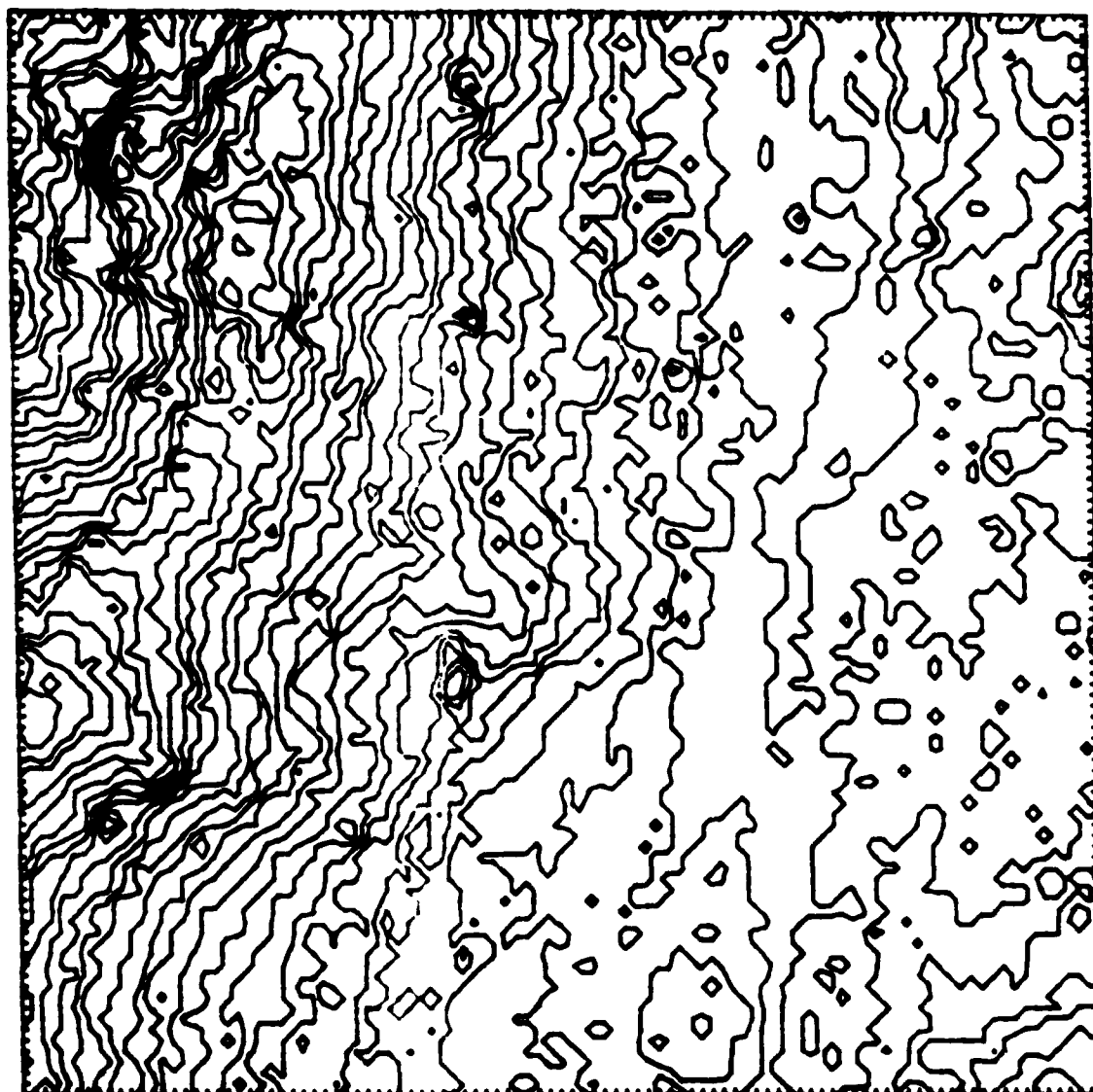
CONTOUR AFTER RES 18
File: CON18.PSC Array has 28 rows and 28 columns
Minimum: 122 Maximum: 131 Interval: .8 Density: 18

Figure 27. Contour Plot after Res 18



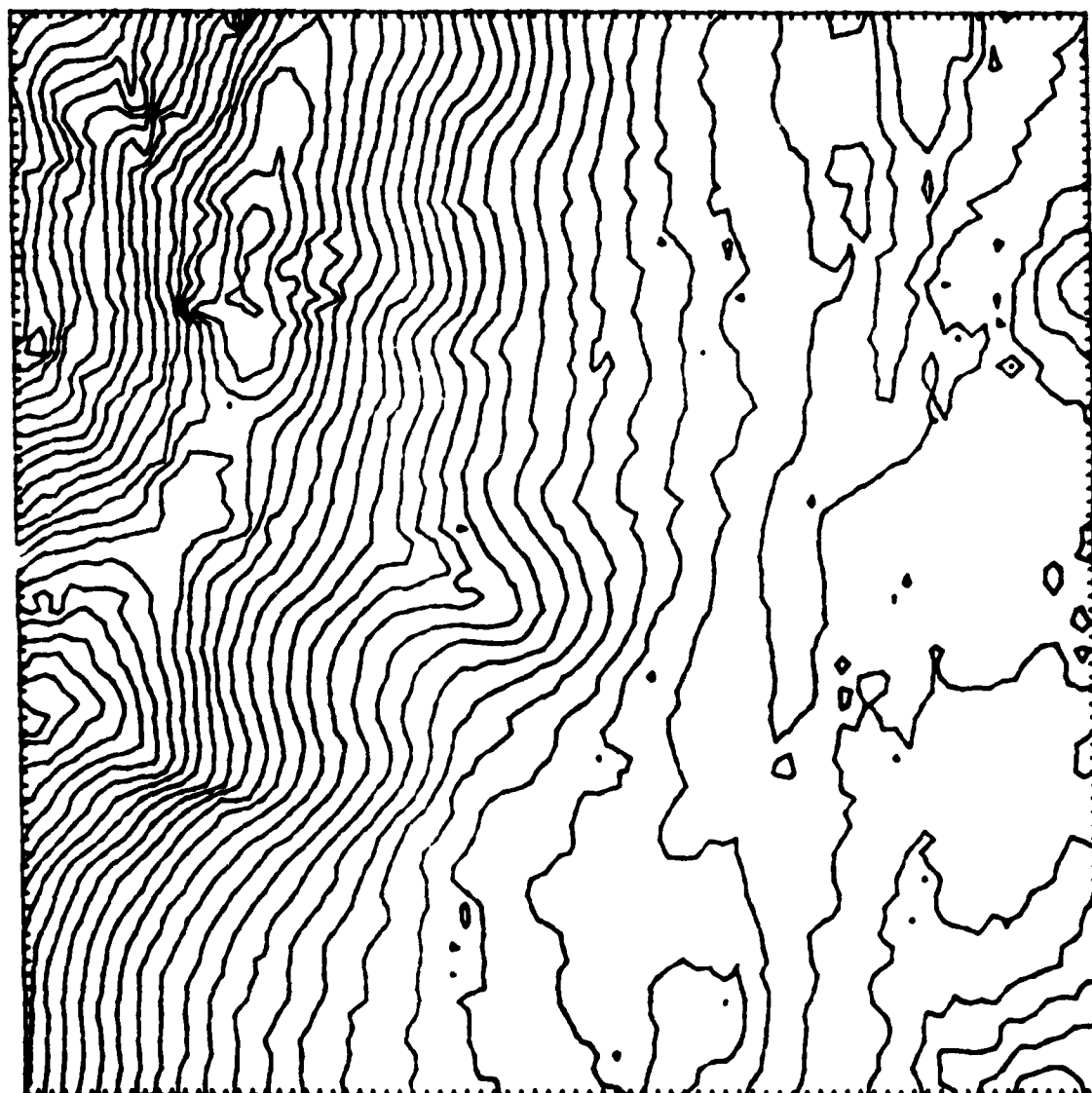
CONTOUR AFTER RES 6
Files: CONE.ASC Array has 60 rows and 60 columns
Minimum: 113 Maximum: 148 Interval: .984205714286 Density: 20

Figure 32. Contour Plot after Res 6



FINAL CONTOUR FROM GRAY SCALE MATCH
File: CON1.ASC Array has 181 rows and 181 columns
Minimum: 97 Maximum: 153 Interval: 1.00000000007 Density: 30

Figure 33. The Final Contour Plot



ETL CONTOUR
Files: C21800 Array has 91 rows and 91 columns
Minimum: 4218 Maximum: 5395 Interval: 37.8 Density: 38

Figure 34. The Calculated Contour from ETL

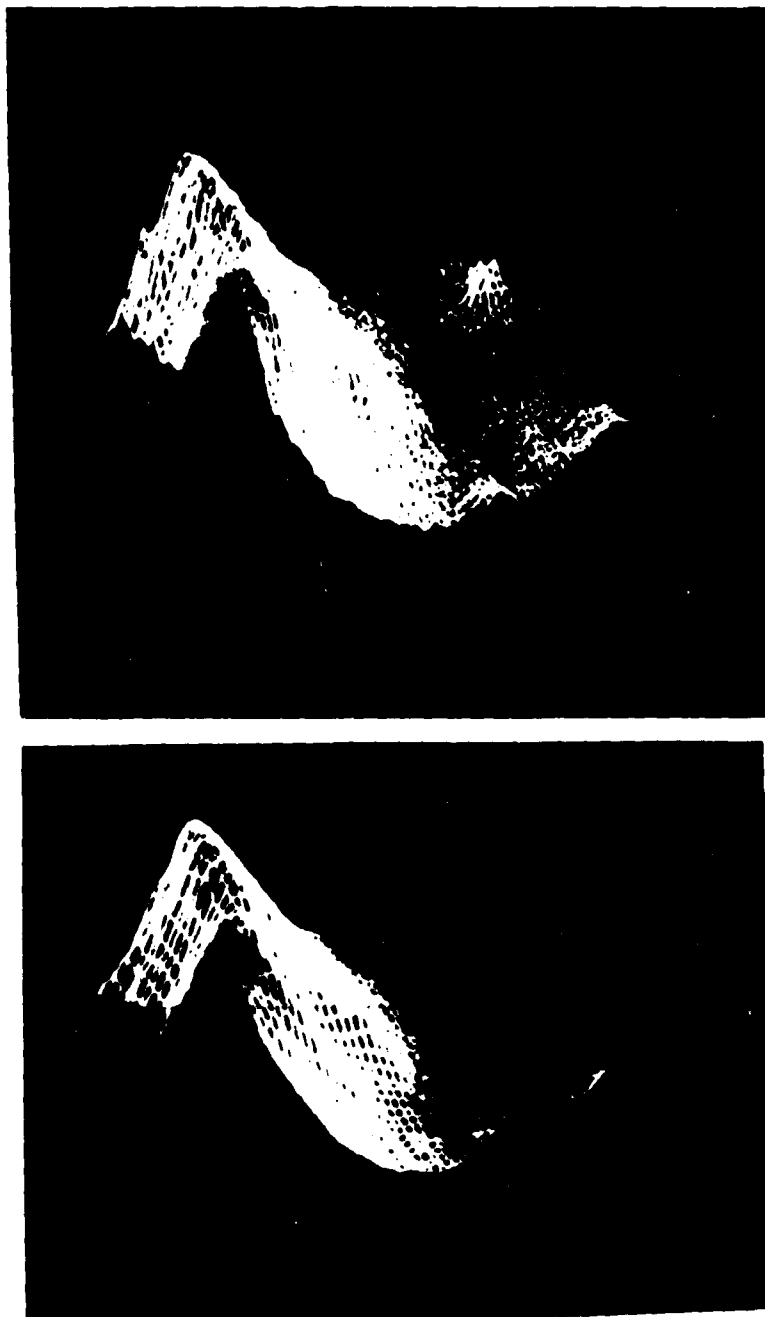


Figure 35. A Surface Plot Comparison

